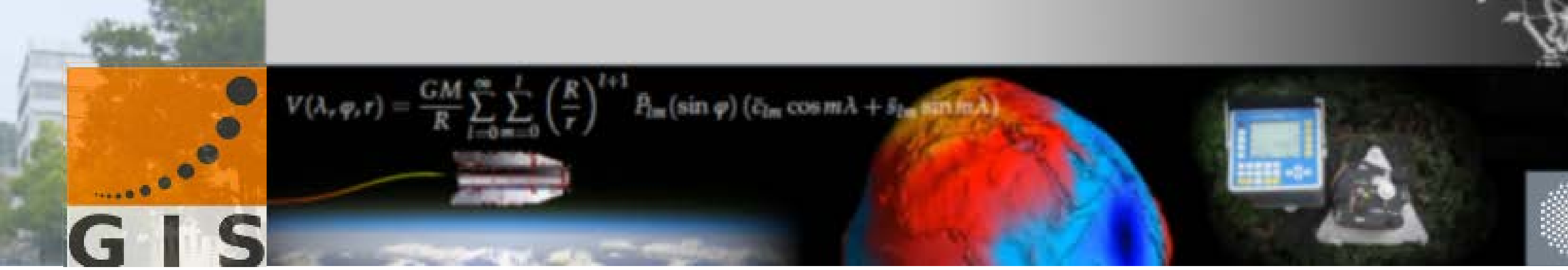

UNIVERSITÉ DU LUXEMBOURG

Second Workshop of DAAD Thematic Network
Modern Geodetic Space Techniques for Global Change Monitoring

Mass Balance Computation in the Space Domain Using GRACE Data

Jinyuan WANG, Wolfgang KELLER

GMB

Gravimetric mass balance (GMB) is important for climatological applications

E.g. Recent contributions of glaciers and ice caps to sea level rise

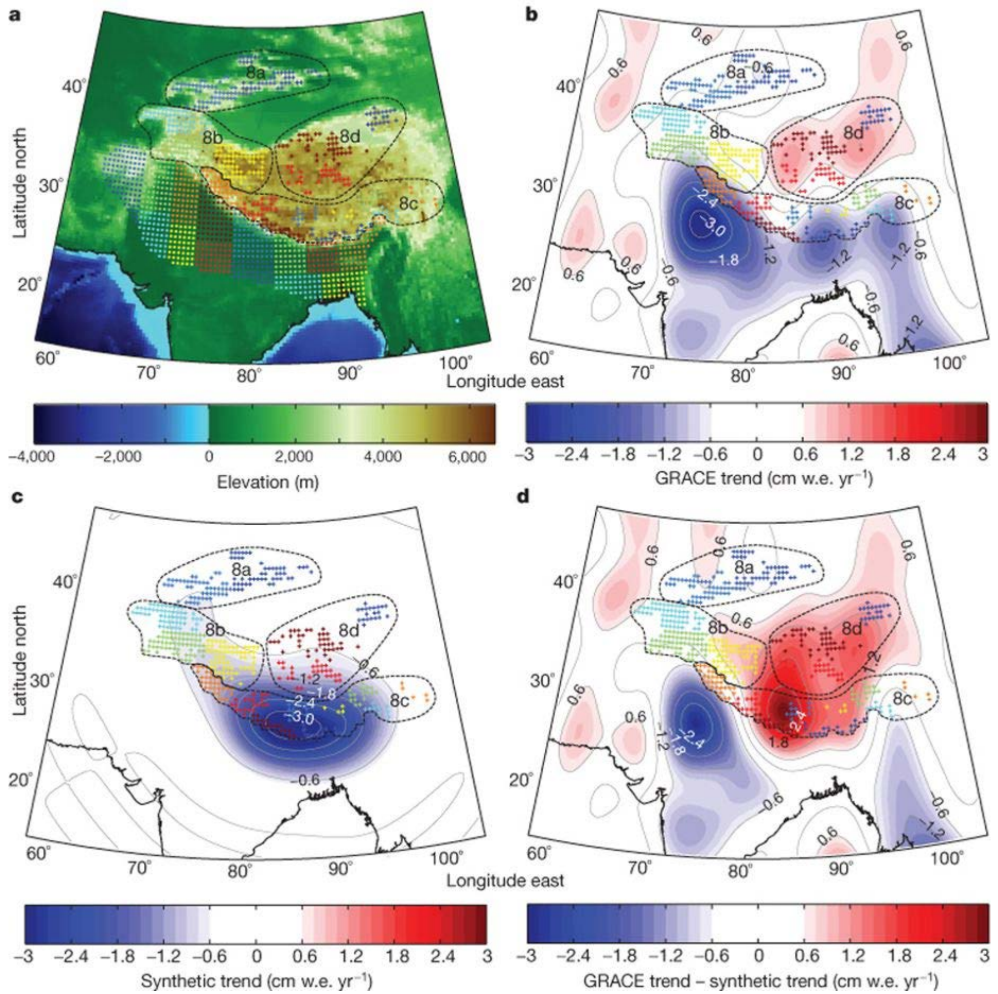

T Jacob *et al*. 2012

High mountain Asia mass balance determination

GMB

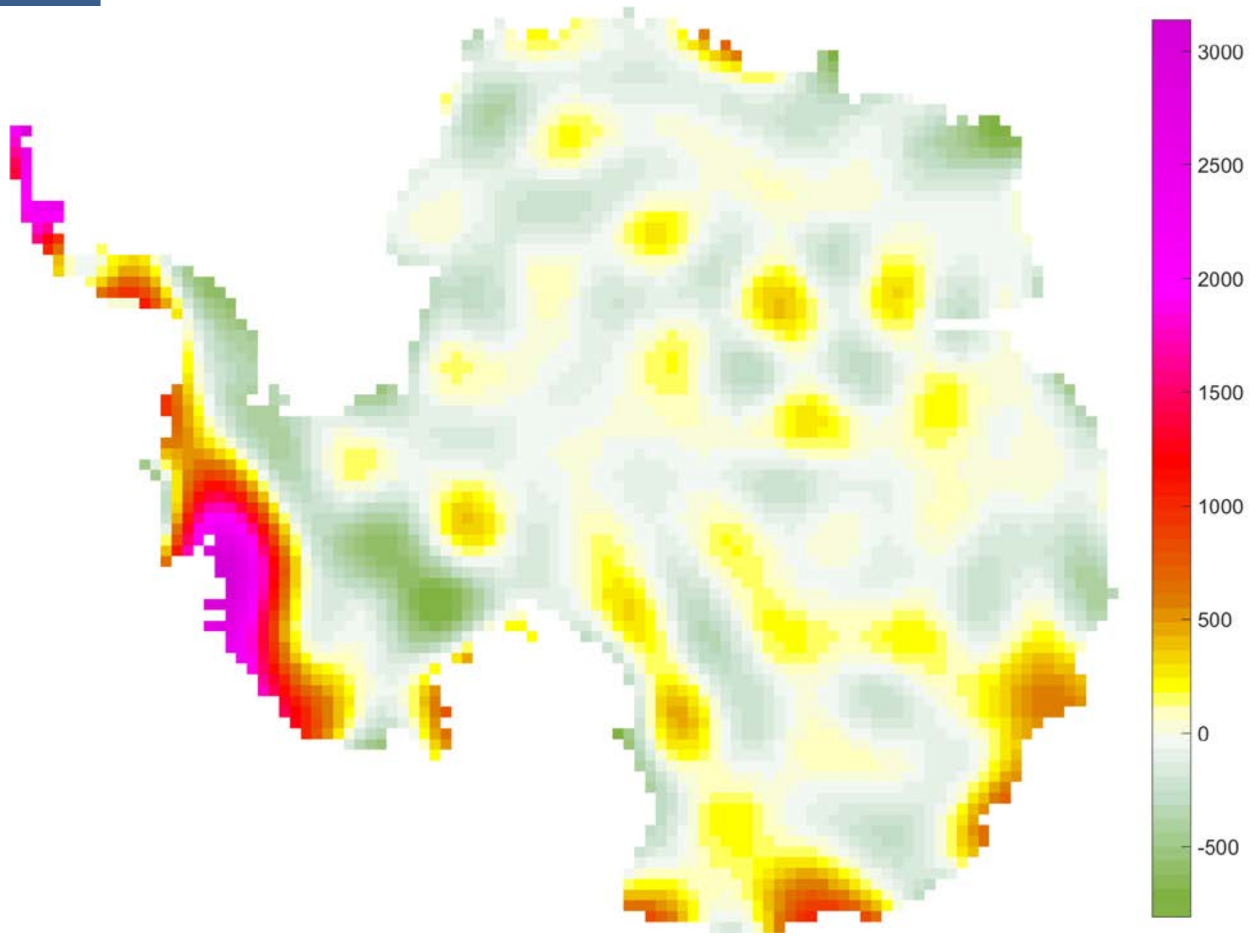

GMB of the Antarctic Ice Sheet on April 2002, unit: kg/m², area: 2217-2642 km²
relative to a modelled reference value, defined to be the GRACE-derived mass as of 2009-01-01

Groh, A., & Horwath, M. (2016)

GMB

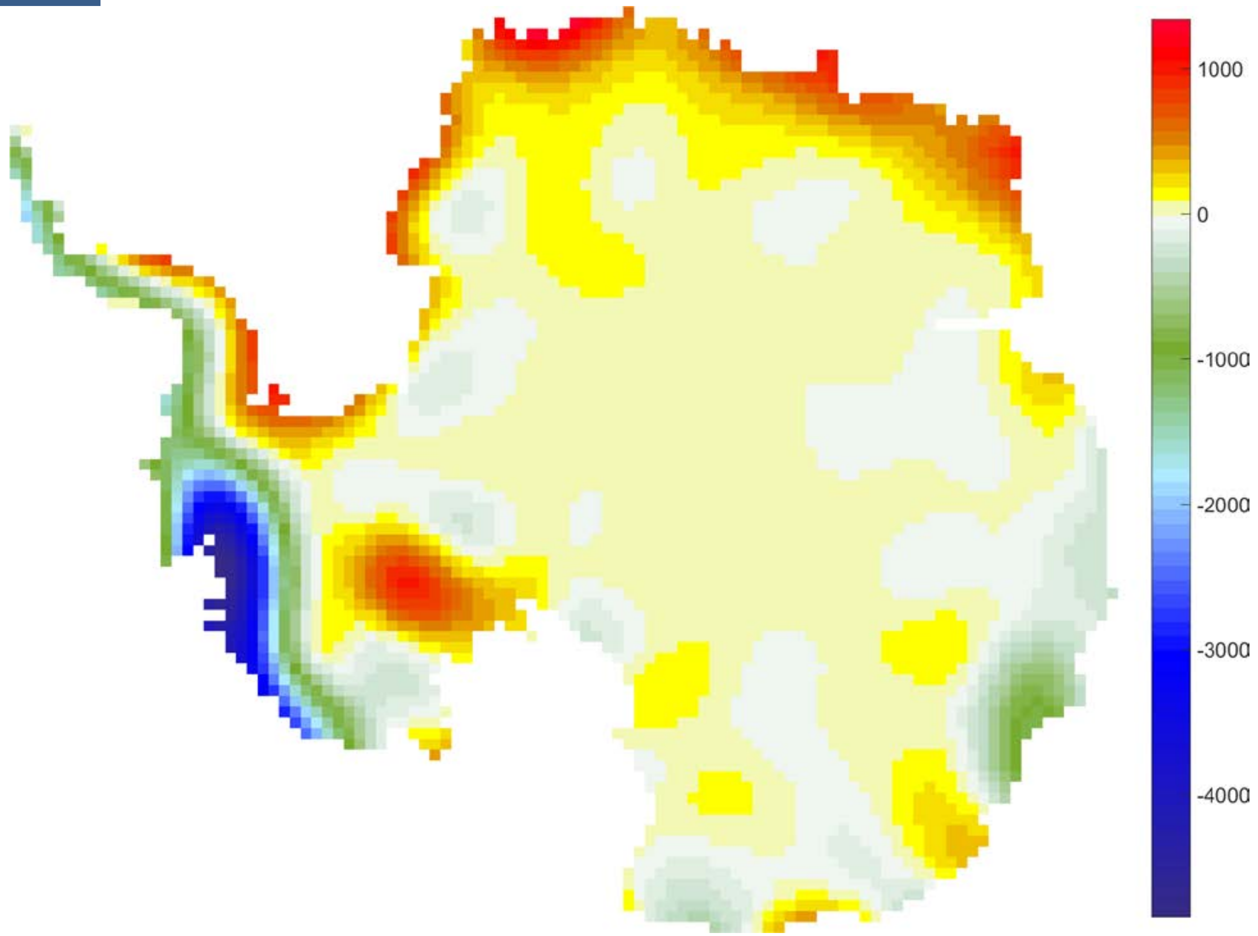

GMB of the Antarctic Ice Sheet on July 2016, unit: kg/m^2, area: 2217-2642 km^2
relative to a modelled reference value, defined to be the GRACE-derived mass as of 2009-01-01

Groh, A., & Horwath, M. (2016)

GMB Observation

- Gravimetry mass balance (GMB) cannot be directly observed from the space
- Only the change of Stokes coefficients can be observed

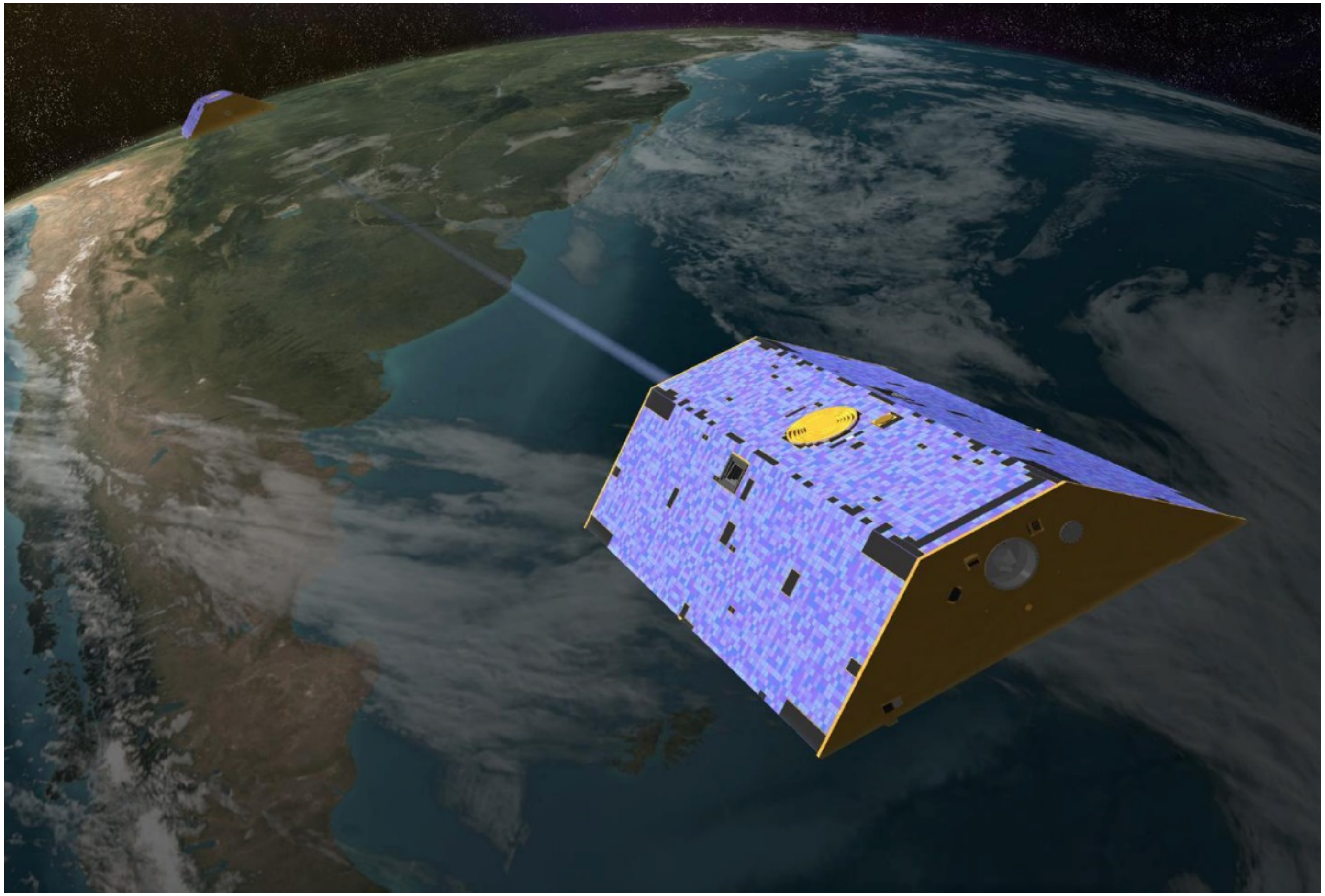

https://www.nasa.gov/mission_pages/Grace/multimedia/pia04236.html#.WyVJKEQV9gM

GMB Computation

How to compute the mass balance (MB) using the Stokes coefficients?

MB within an area B is the integral of the density change:

$$\Delta m_{\mathrm{B}} = \int_{\mathrm{B}} \Delta\sigma \, \mathrm{dA}$$

The density change at a certain point can be derived from the change of the Stokes coefficients, via spherical harmonics (Wahr and Molenaar 1998):

$$\Delta\sigma(\varphi, \lambda) = \frac{R\,\rho_{\mathrm{E}}}{3} \sum_{l=0}^{\infty} \sum_{m=0}^{l} \overline{Y}_{lm}(\varphi, \lambda) \Delta c_{lm}$$

- Even if $\Delta\sigma$ can be given point-wisely, the value would be meaningless
- Applying the spatial averaging (integration) for $\Delta\sigma$ within an target area is necessary

EWH

Examples of the global density change converted to the equivalent water height

- Noises, “stripes” can be seen

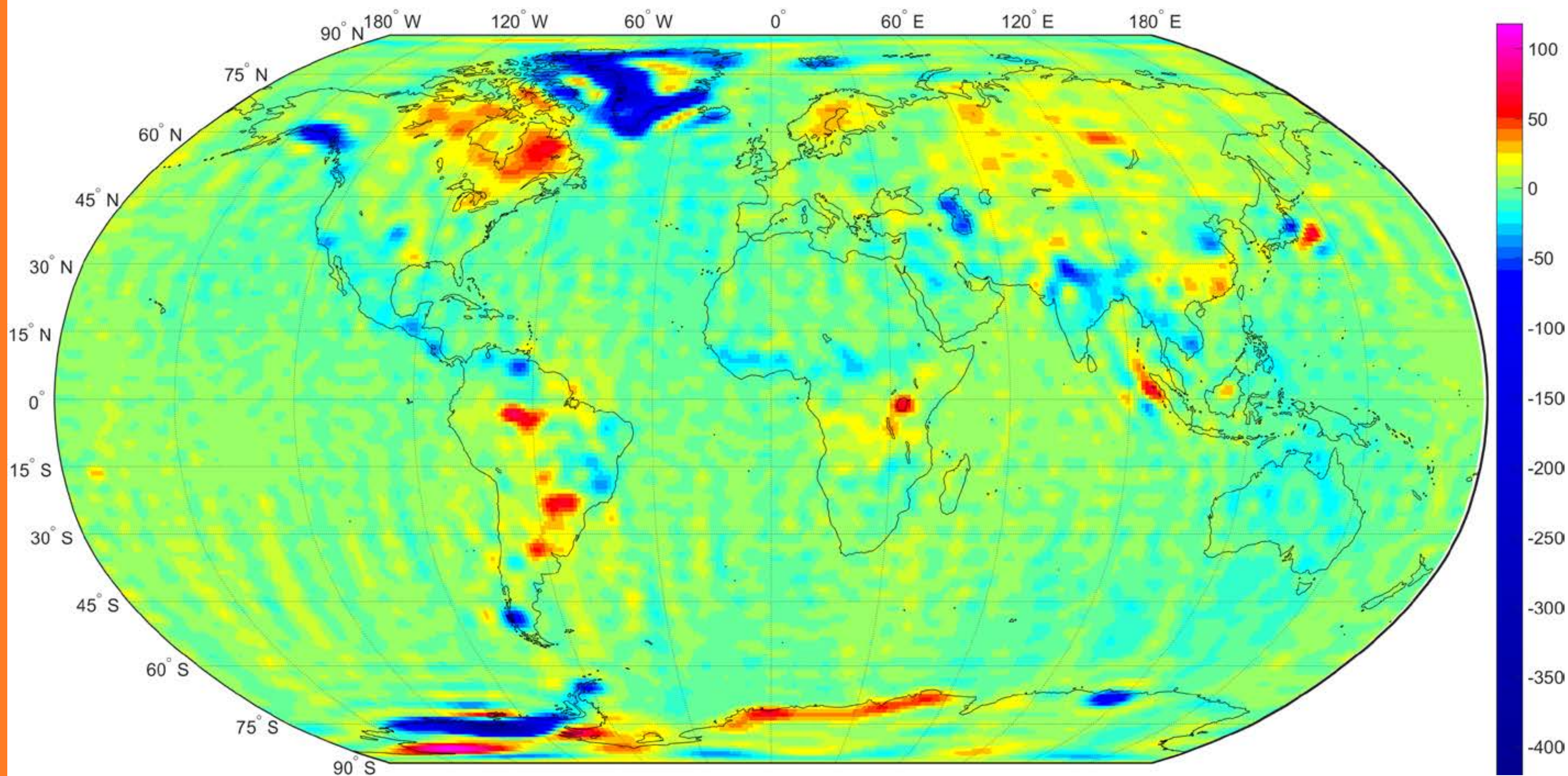

Global EWH change on December 2016, **non filter** applied (unit: cm)

based on the monthly solution from CNES/GRGS, refence value: the mean between 2002 and 2013

EWH

Examples of the global density change converted to the equivalent water height

- Spatial resolution of MB recoveried from GRACE is around 200 km
- MB cannot be a point measurement, but a spatial average (Swenson & John 2002)

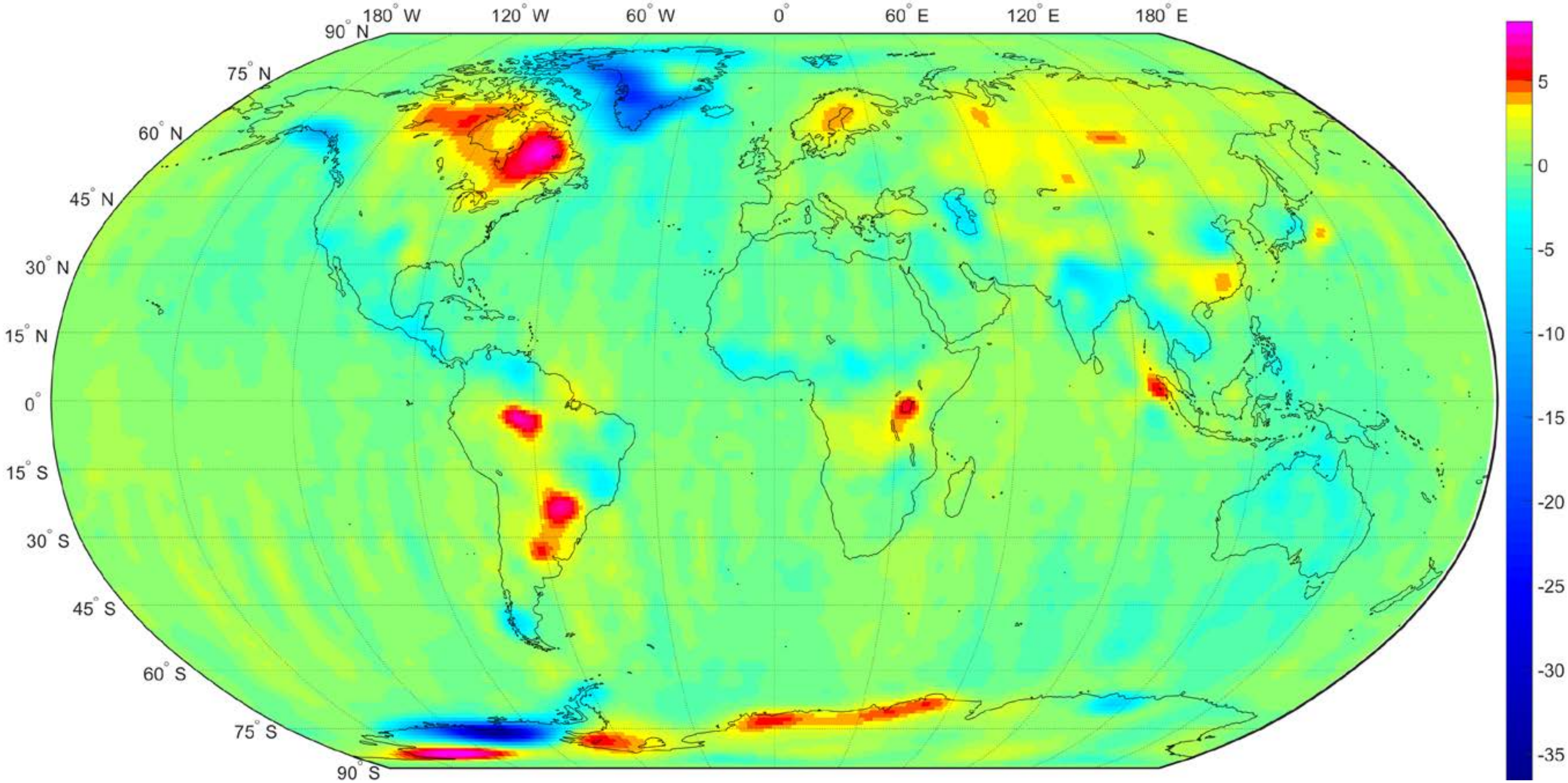

Global EWH change on December 2016, **Gaussian filter** applied (unit: cm)
based on the monthly solution from CNES/GRGS, refence value: the mean between 2002 and 2013

GMB Computation

Traditional approach – a spectral/frequency-domain method

- Applying the spatial averaging kernel (Characterictic function of the area)

(Swenson & John 2002)

$$\chi_{lm} = \int_{\mathrm{B}} \overline{Y}_{lm}(\varphi,\lambda)\,\mathrm{dA} \quad \Longrightarrow \quad \Delta m_{\mathrm{B}} = \frac{R\,\rho_{\mathrm{E}}}{3}\sum_{l=0}^{\infty}\sum_{m=-l}^{l}\chi_{lm}\Delta c_{lm}$$

- The integration of the Legendre functions is involved
- Using recursive formulas, known as Paul's recursion (Paul 1978), to compute χ_{lm}

$$\bar{I}_{lm}(t_1,t_2) = \int_{t_1}^{t_2}\overline{P}_{lm}(t)\,\mathrm{d}t\ , \qquad \text{with } t = \sin\varphi$$

Disadvantages:

- Longer mantissa for the computation $\Longrightarrow$ significantly lose efficiency
- Instability, especially in the latitude range of 40˚N - 70˚N and 40˚S - 70˚S

Alternative

Instead of compute the integration with a lot of recursions, can we make a direct numerical evaluation of the integration?

- Newly proposed method: Space-domain approach using numerical quadrature

Comparison between these two approaches

- Frequency domain
- Space domain

For the computation of

- Integral of the Legendre functions (ILF): $\int_{t_1}^{t_2} \overline{P}_{lm}(t)\,\mathrm{d}t$
- MB: $\int_{\mathrm{B}} \Delta\sigma\,\mathrm{dA}$

In term of

- Precision of the results
- Stability of the results
- Computational efficiency

Reference Data Set

In order to evaluate the precision and determine the stability, a reference data set is needed, it requires:

- Precision: same as the length of the "double-float" number
- No instabilities

However...

- For ILF, we do not have a complete reference data set elsewhere
- For MB, Stokes coefficients contribute error, different filtering and data source lead to different result

Luckily...

- We can use sufficiently long mantissa (≥ 108 significant digits for $l_{\max} = 100$) to compute ILF in the spectral domain, the result is accurate
- Using this ILF, we can compute MB and treat it as the true value

Spectral Domain

How is MB computed in the spectral domain?

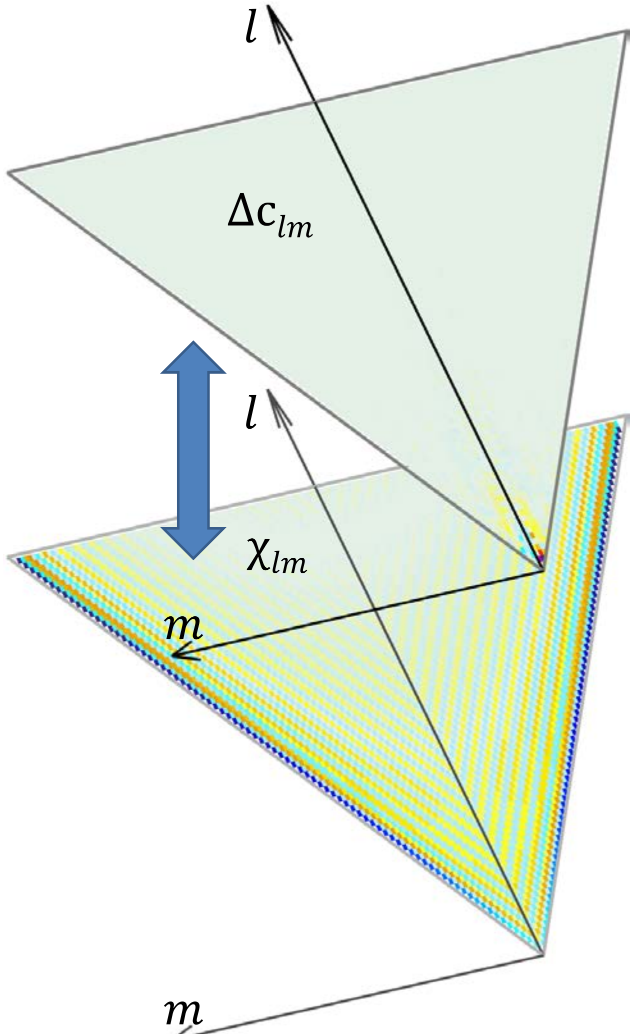

- The Stokes coefficients and the characteristic function are multiplied element-wisely
- For patches with the same latitude range, the characteristic function only needs to be computed once

Disadvantages:

- Computationally inefficient: each patch has different characteristic function
- **Instability**

Instability

Minimum precision of ILF computed with double float number integrated every 5°, presented in the number of significant digits

Integral Range	0° – 5°N	5°N – 10°N	10°N – 15°N	15°N – 20°N	20°N – 25°N	25°N – 30°N	30°N – 35°N	35°N – 40°N	40°N – 45°N
Precision	10	10	10	11	10	11	8	7	**4**
Integral Range	**45°N – 50°N**	**50°N – 55°N**	**55°N – 60°N**	**60°N – 65°N**	**65°N – 70°N**	**70°N – 75°N**	**75°N – 80°N**	**80°N – 85°N**	**85°N – 90°N**
Precision	**0**	**E**	**E**	**E**	**E**	**7**	**8**	**11**	**11**

- Same condition in the Southern Hemisphere
- Optimized recursion formula applyed near the Pole
- E: (wrong values occur), indicates low precision and instabilities within the latitude range from 40°N to 70°N, starts from the integral of the tesseral harmonics

Instability

Precision of some representative values of $\bar{I}_{ll}$ (integrals of tesseral harmonics) presented in the number of significant digits

l \ φ_1 / φ_2	40°N / 45°N	45°N / 50°N	50°N / 55°N	55°N / 60°N	60°N / 65°N	65°N / 70°N
0	15	15	15	15	15	15
10	15	14	14	13	12	10
20	13	12	12	10	9	7
30	12	11	9	8	6	4
40	11	9	8	5	3	**0**
50	11	8	6	3	**0**	**E**
60	9	6	4	**0**	**E**	**E**
70	8	5	2	**E**	**E**	**E**
80	7	3	**0**	**E**	**E**	**E**
90	6	2	**E**	**E**	**E**	**E**
100	5	**0**	**E**	**E**	**E**	**E**

- Instability starts from the **Middle latitude**
- Due to the property of recursion – later results depend on the previous results, errors from the integral of tesseral harmonics bring the instabilities to the final result

Mantissa

Minimum mantissa required for the recursive algorithm

for the computation of ILF up to 100 degree, presented in the number of significant digits

φ_1 ⋯ φ_2	0° ⋯ 5°N	5°N ⋯ 10°N	10°N ⋯ 15°N	15°N ⋯ 20°N	20°N ⋯ 25°N	25°N ⋯ 30°N	30°N ⋯ 35°N	35°N ⋯ 40°N	40°N ⋯ 45°N
Mantissa	7	7	7	7	7	7	7	8	12
φ_1 ⋯ φ_2	45°N ⋯ 50°N	50°N ⋯ 55°N	55°N ⋯ 60°N	60°N ⋯ 65°N	65°N ⋯ 70°N	70°N ⋯ 75°N	75°N ⋯ 80°N	80°N ⋯ 85°N	85°N ⋯ 90°N
Mantissa	15	19	24	30	38	47	60	77	108

- Shorter mantissa required at lower latitudes
- The number differs when:
  - $l_{\max}$ changes
  - The integral range changes

When the mantissa is sufficiently long, would the results be perfect?

χ-check

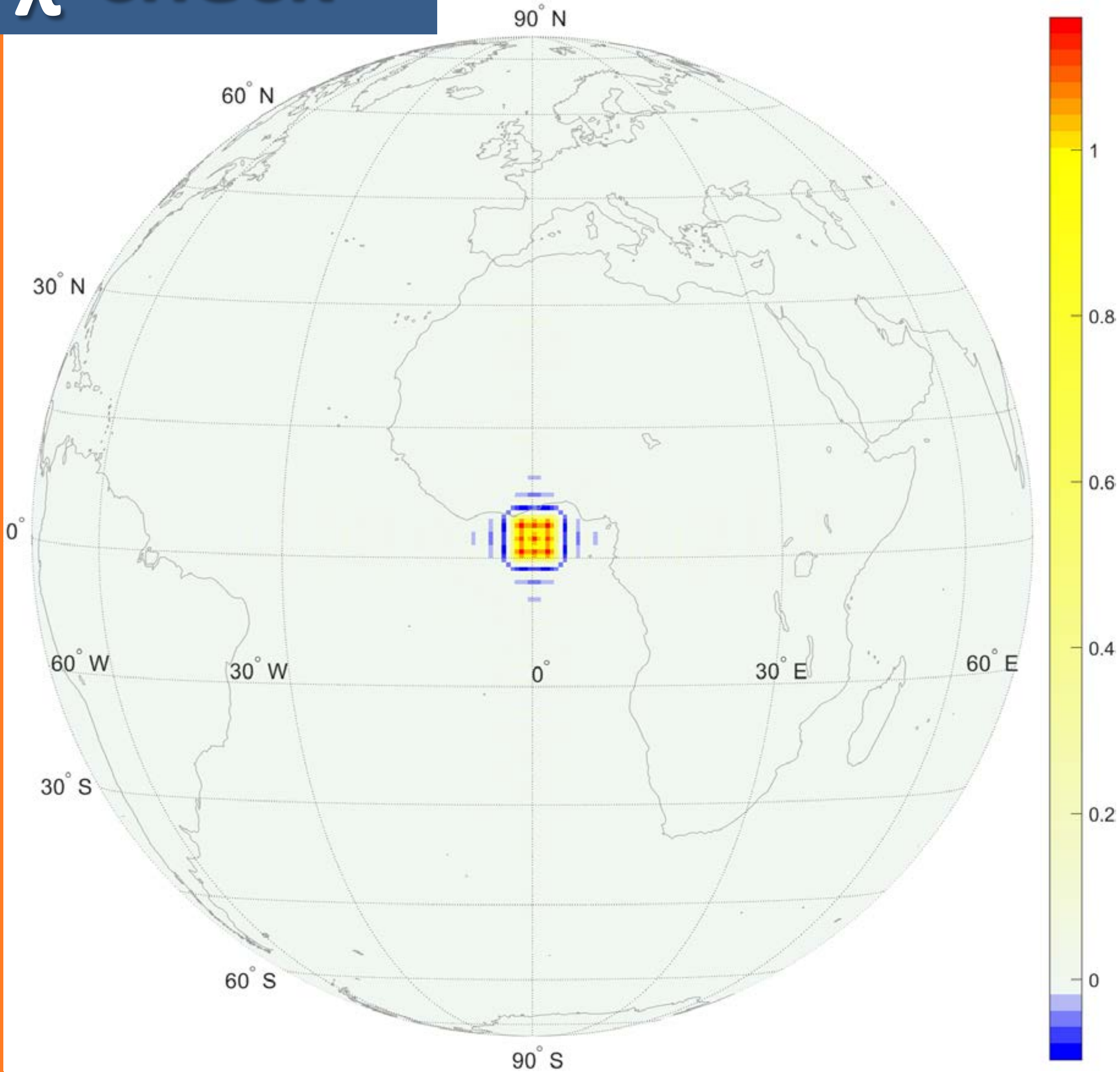

latitude range: 0° - 5°N, longitude range: 2.5°W - 2.5°E

- Ideally:

$$\chi_{\mathrm{B}}(\xi) = \begin{cases} 1 & \text{for } \xi \in \mathrm{B} \\ 0 & \text{for } \xi \notin \mathrm{B} \end{cases}$$

- The equiangular patch is in the "blue ring"
- Inside the patch, is almost 0
- Outside the patch there are negative values forming the disturbance (waves)
- Due to truncation

$$\sum_{l=0}^{\infty} \sum_{m=-l}^{l} \chi_{lm} \Delta c_{lm} \qquad \sum_{l=0}^{100} \cdots$$

χ-check

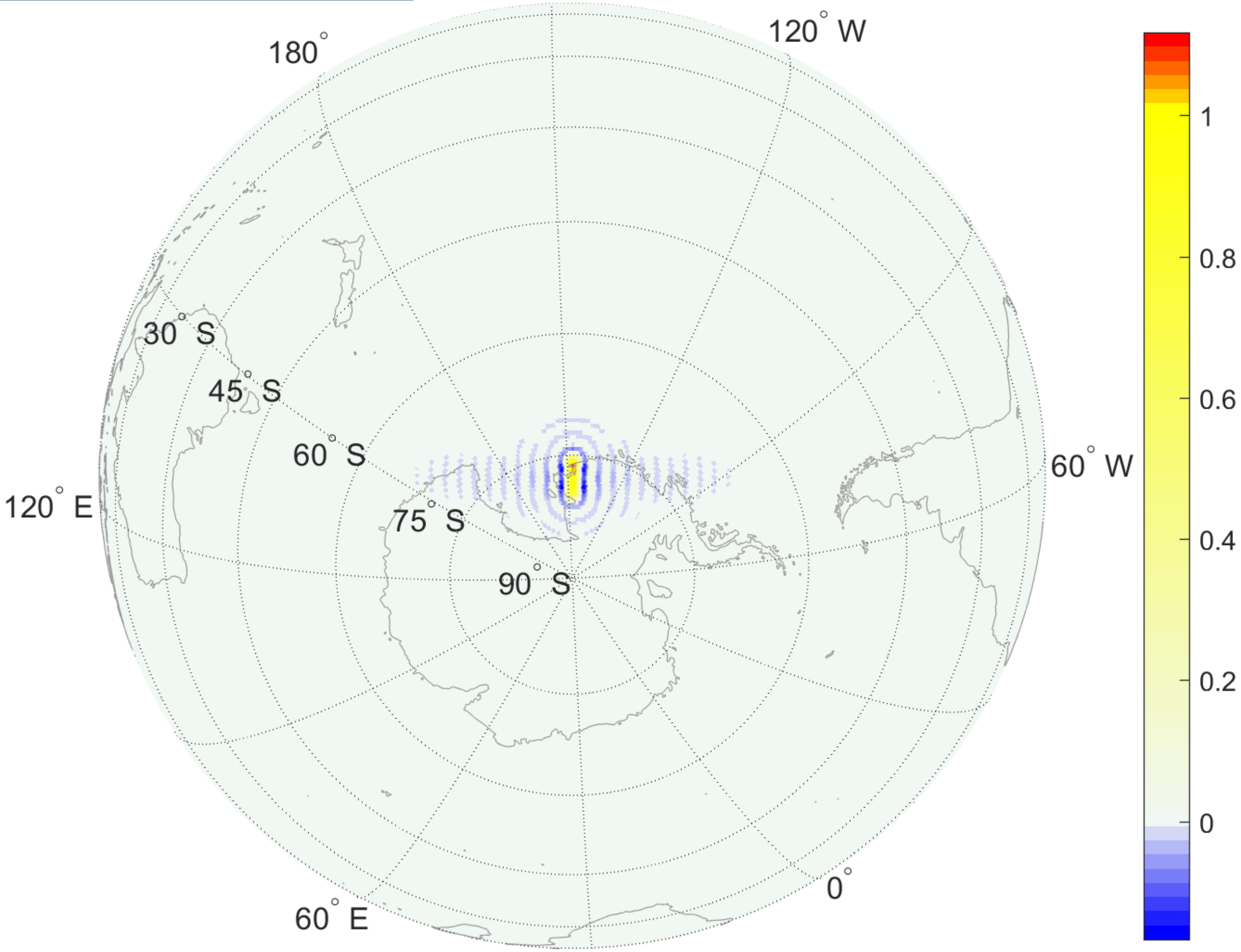

- More waves approaching the Pole, indicating the truncation has stronger influence
- The **exact integration** of an **approximate characteristic function** does not perform perfectly

latitude range: 10°S - 15°S, longitude range: 150°W - 145°W

Numerical Quadrature

Newton-Cotes Quadrature

$$F(x_1, x_2, y_1, y_2) \triangleq \int_{y_1}^{y_1} \int_{x_1}^{x_2} f(x, y)\, \mathrm{d}x\, \mathrm{d}y \approx k_x\, k_y\, h_x\, h_y \sum_{j=0}^{J_x} v_{x_j}\, f_{x_j} \cdot \sum_{j=0}^{J_y} v_{y_j}\, f_{y_j}$$

Rafelski, (1984)

Visualization of the weights of Bool's rule distributed on an equiangular patch

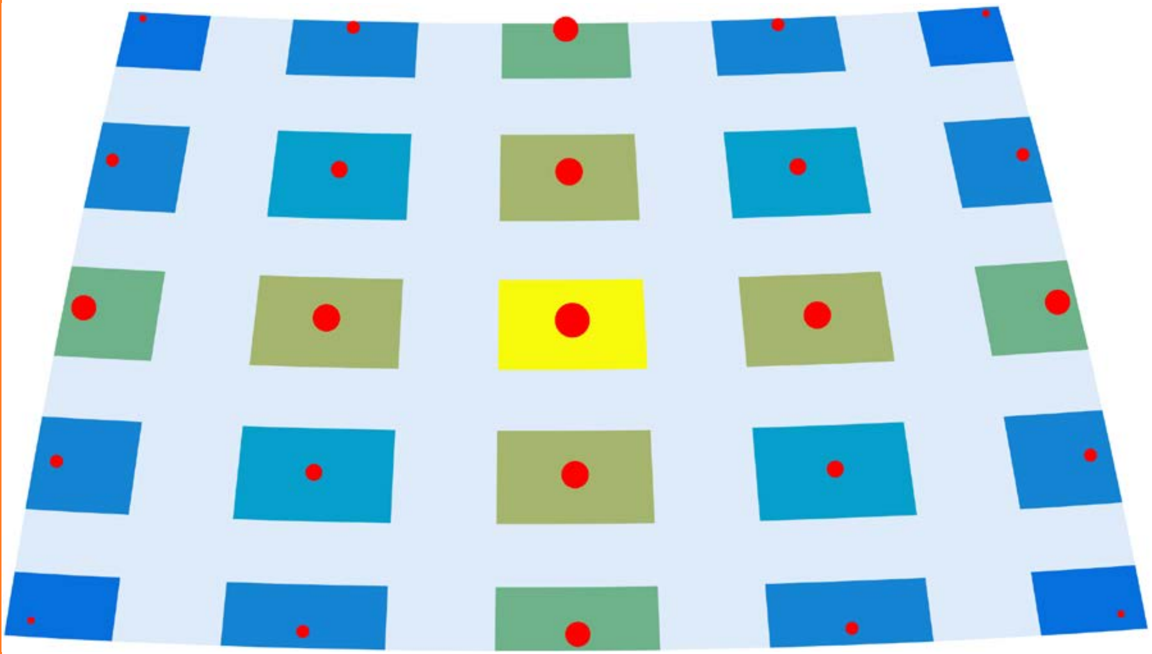

- The location of the weights is evenly distributed, "linear"
- The value of the weights increases from the edge to the center
- For ILF computation, it estimates the integration of the exact characteristic function

The size of the red dots (or the brightness of the colorful patches) indicates:

- where the evaluation takes place
- how high the weight is

Numerical Quadrature

Gaussian Quadrature

$$G(x_1, x_2, y_1, y_2) \triangleq \int_{-1}^{1}\int_{-1}^{1} g(x,y)\,\mathrm{d}x\,\mathrm{d}y \approx k_x\,k_y \sum_{j=0}^{J_x} w_{x_j}\,g_{x_j} \cdot \sum_{j=0}^{J_y} w_{y_j}\,g_{y_j}$$

Visualization of the weights distributed on an equiangular patch

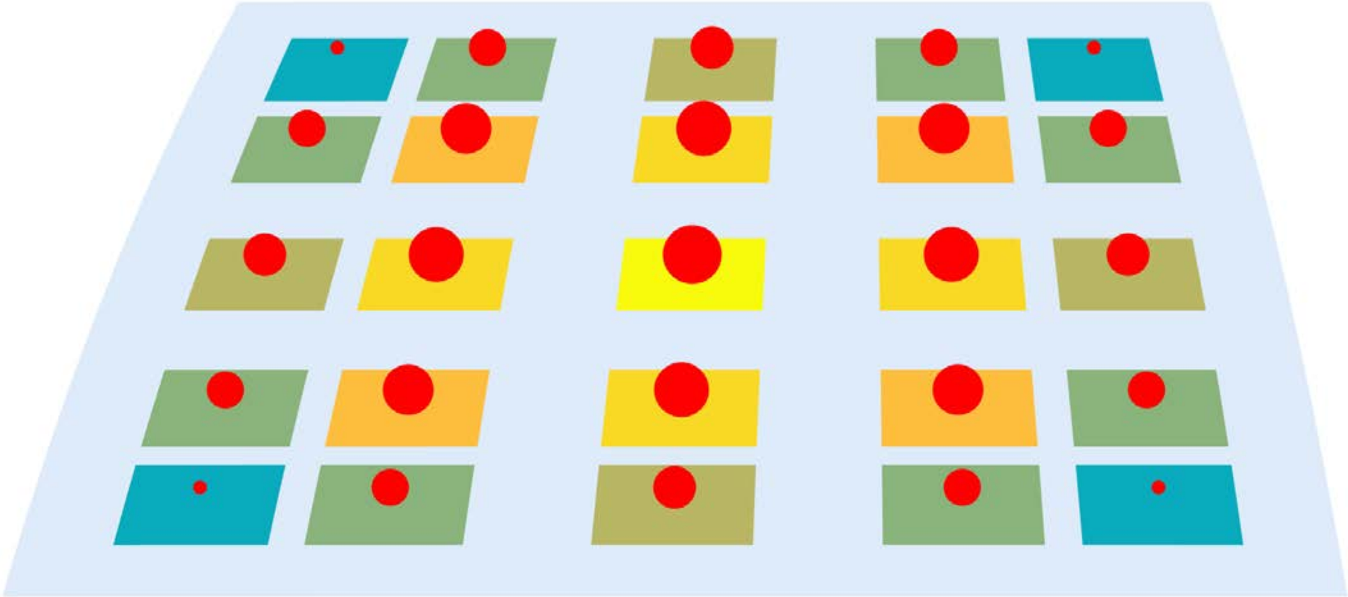

- The location of the weights is not evenly distributed, "nonlinear"
- The value of the weights also increases from the edge to the center
- But the distribution gets denser towards the edge
- Requires fewer evaluations than commonly used Newton-Cotes quadratures

Comparison

Minimum possible number of points required for two numerical quadrature rules ILF computation, for different latitude range with the size of 5°

Latitude Range	Bool's Rule	Gaussian Quadrature
0° - 20°N	57	8
20°N - 30°N	57	9
30°N - 40°N	61	9
40°N - 45°N	69	9
45°N - 70°N	85	9
70°N - 75°N	85	10
75°N - 80°N	117	12
80°N - 85°N	169	16
85°N - 90°N	341	20

- In general, Gaussian quadrature requires less than half as many evaluations as commonly used Newton-Cotes quadrature does

Comparison

Efficiency comparison of two numerical quadrature rules
for ILF computation from 90°S to 90°N

Name of the rule	Number of Points (nodes)	Averaged Computational Time
Boole's Rule	341	6.1×10^{-2} s/IR
Gaussian Quadrature	20	4.3×10^{-3} s/IR

IR: Integral Range (with the size of 5° along the latitude)

- For space-domain approach, Gaussian quadrature has better performance
- Gaussian quadrature computes hundreds times as fast as Bool's rule does

Comparison

Efficiency for ILF computation among listed approaches

Approach	Spectral Domain Sufficient Mantissa	Space Domain Boole's Rule	Space Domain Gaussian quadrature
Averaged Computational Time	1.7×10^{2} s/IR	6.1×10^{-2} s/IR	4.3×10^{-3} s/IR

Sufficient long Mantissa: 89 significant digits, for $l_{\max} = 80$

Efficiency for the global GMB computation

between the spectral-domain approach and the space-domain approach

Approach	Spectral Domain Sufficient Mantissa	Space Domain Gaussian quadrature
Averaged Computational Time	4.2×10^{1} s/B	5.2×10^{-2} s/B

B: An equiangular patch on the Earth's surface with a size of $5°\times5°$

Reference

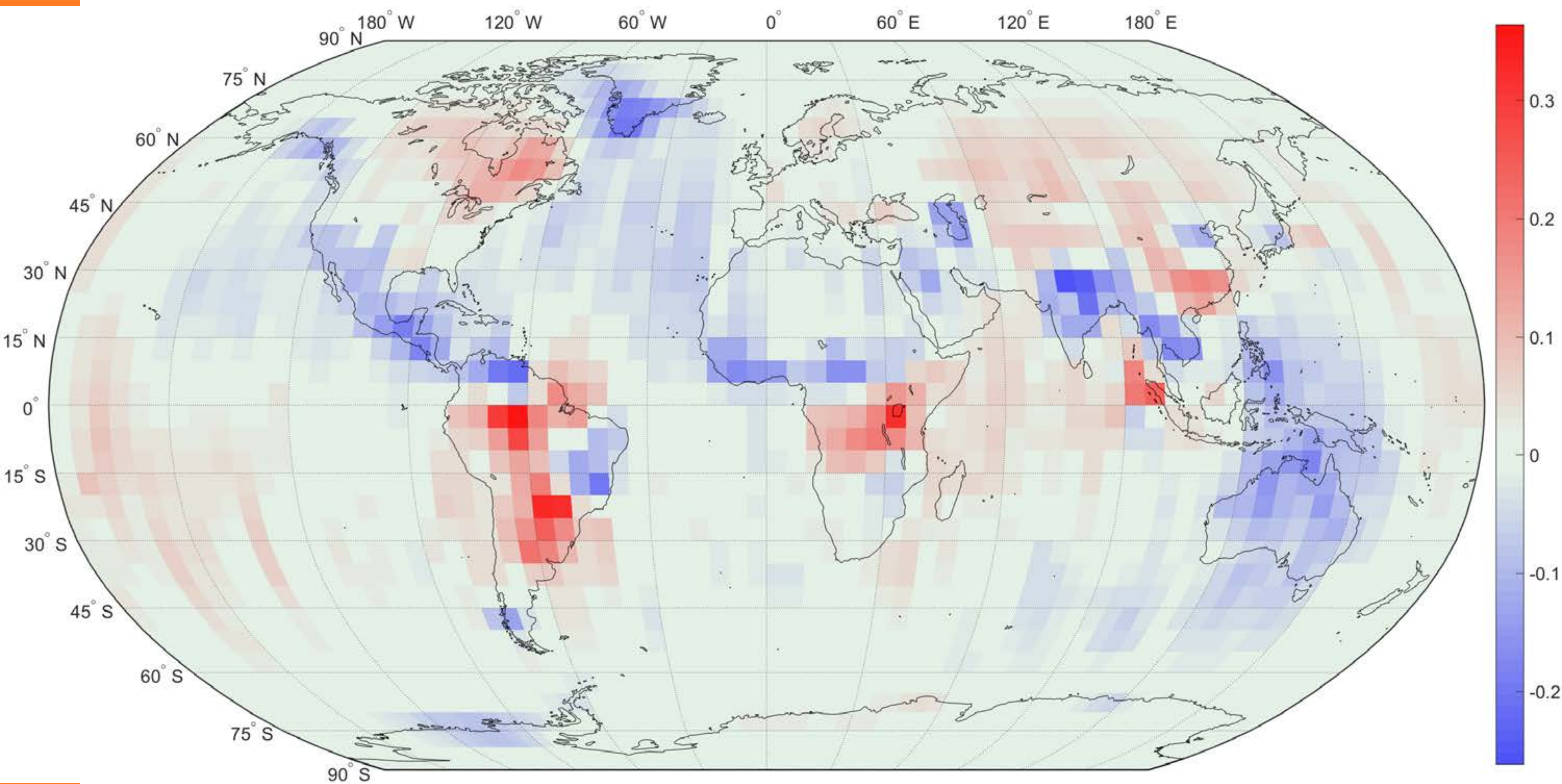

Global GMB on December 2016, unit: Gt

computed in the spectral domain with sufficiently long mantissa (89 significant digits)

Space Domain

No visible difference

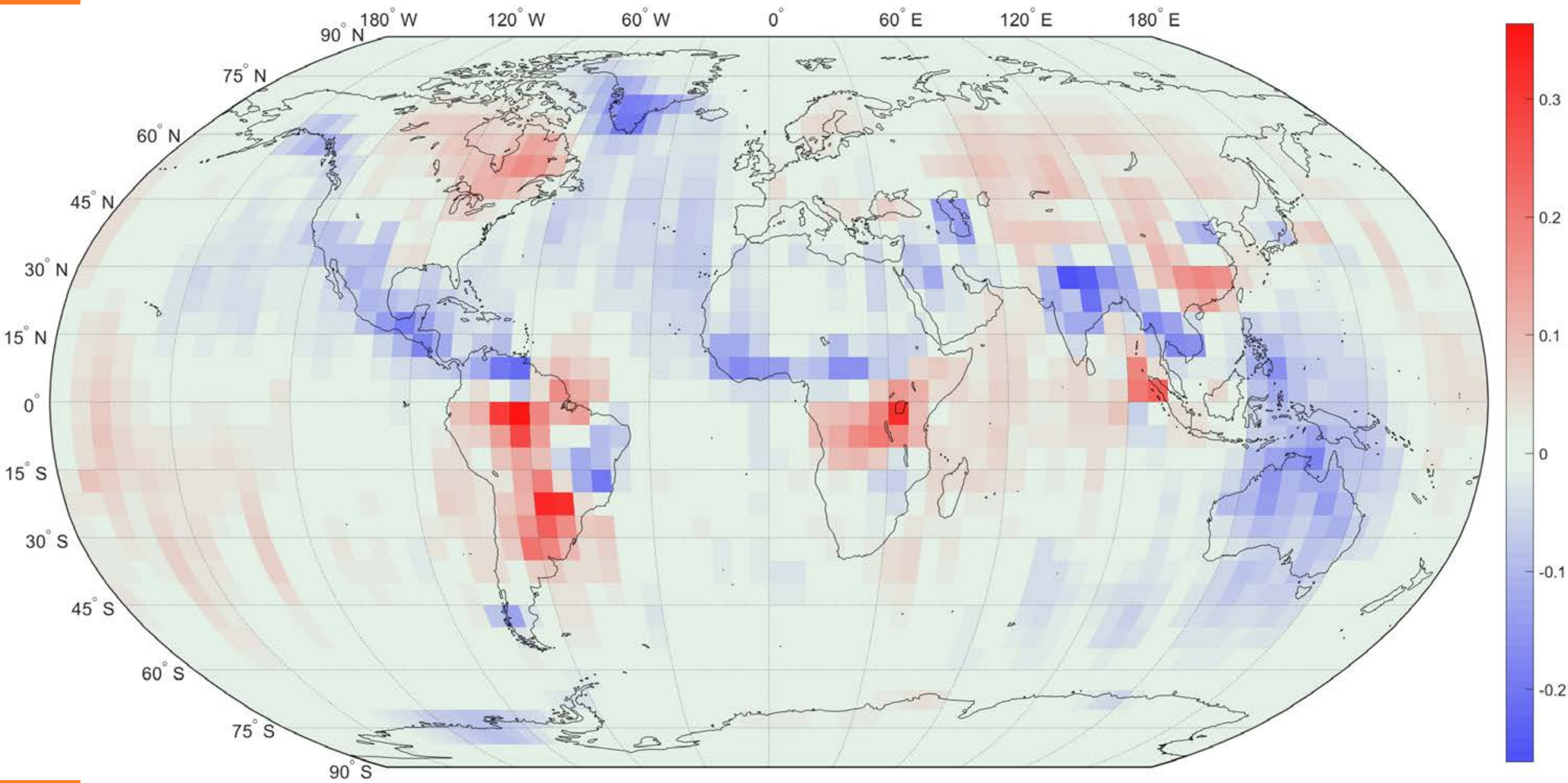

Global GMB on December 2016, unit: Gt
computed in the space domain using Gaussian quadrature (20 points)

GMB Precision

Independent on the latitude

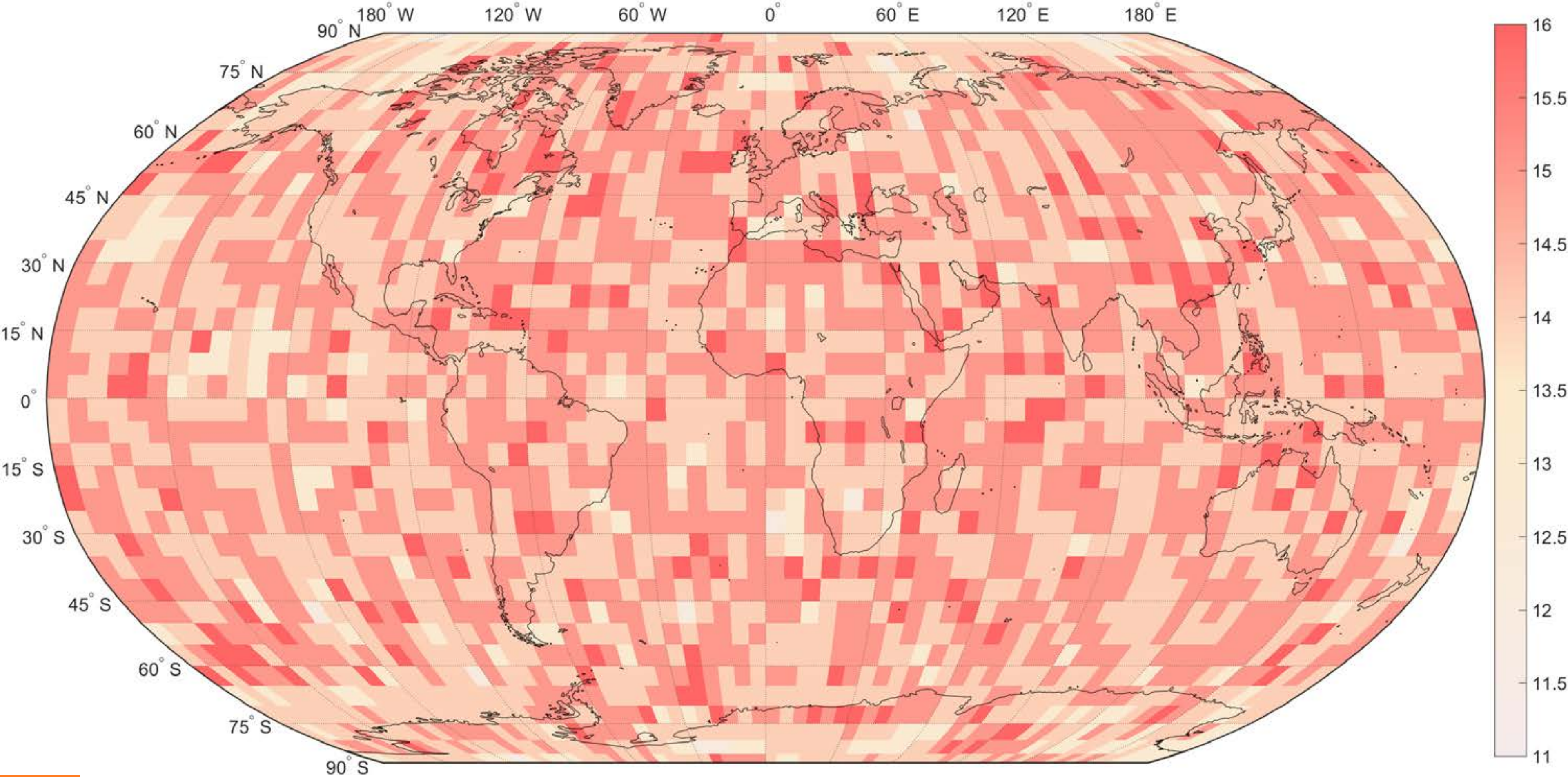

Average precision of the global GMB from April 2002 to July 2016 computed in the space domain using Gaussian quadrature (20 points) presented in the number of significant digits

GMB Precision

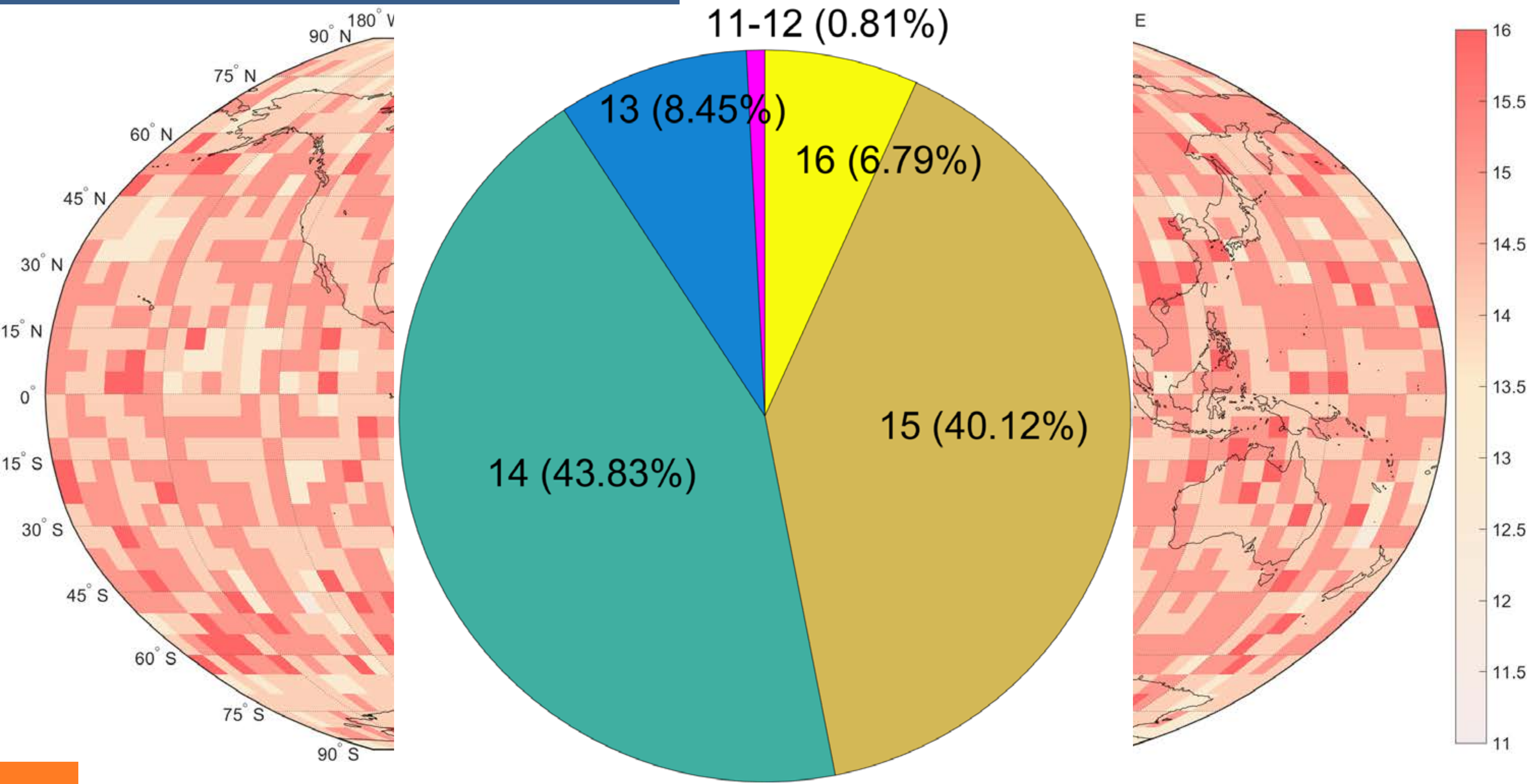

- The goal is to reach **6** significant digits
- **100%** of the computed GMB reaches the goal, **46%** (almost) **identical** to the reference
- Worst case (less than **1%**): losing **4** to **5** significant digits

Conclusion

Precision:

- Spectral domain: precise only using sufficiently long mantissa
- Space domain: as precise as the spectral-domain approach, by choosing an appropriate number of evaluation points

Stability:

- Spectral domain: Instability happens when the mantissa is not sufficiently long
- Space domain: Stable

Efficiency:

- Spectral domain: Not efficient, incredibly slow
- Space domain: Very efficient; Gaussian quadrature is almost 1000 times faster than the spectral-domain approach, and around 100 times faster than commonly used Newton-Cotes quadrature

Others:

- The evaluation of the integration along the longitude direction can be optimized by analytic solution

Outlook

- Apply advanced numerical analysis, e.g. Romberg's method
- The algorithm can be further optimized: at different latitude, the number of the evaluation point for the numerical quadrature differs

Reference

1. Groh, A., & Horwath M. (2016), GMB Product. **URL:** *https://data1.geo.tu-dresden.de/ais_gmb/*
2. Jacob, T. & *et al*. (2012), *Nature* **000**, 1-5, **URL:** *http://dx.doi.org/10.1038/nature10847*
3. Wahr, J., Molenaar, M. & Bryan, F. (1998), 'Time variability of the earth's gravity field: Hydrological and oceanic effects and their possible detection using grace', *Journal of Geophysical Research: Solid Earth* **103**(B12), 30205–30229. **URL:** *http://dx.doi.org/10.1029/98JB02844*
4. CNES/GRGS (2016), Monthly solution of the Stokes coefficients, **URL:** *https://grace.obs-mip.fr/*
5. Swenson, S. & Wahr, J. (2002), 'Methods for inferring regional surface-mass anomalies from gravity recovery and climate experiment (grace) measurements of time-variable gravity', *Journal of Geophysical Research: Solid Earth* **107**(B9), ETG 3–1–ETG 3–13. 2193. **URL:** *http://dx.doi.org/10.1029/2001JB000576*
6. Paul, M. K. (1978), 'Recurrence relations for integrals of associated Legendre functions', *Bulletin Géodésique* **52**(3), 177–190. **URL:** *https://doi.org/10.1007/BF02521771*
7. Rafelski, J. (1984), *Pocketbook of Mathematical Functions*, Verlag Harri Deutsch - Thun.

End

Blood Moon